

1 Supplementary Information: Monitoring Lithiation
2 Gradients in Solid-state Batteries Using *Operando*
3 Neutron Radiography

4 *Patrice Perrenot^{1*}, Lukas Helfen², Ove Korjus², Oskar Thompson¹, Fannie Alloin¹, Claire*
5 *Villevieille^{1*}*

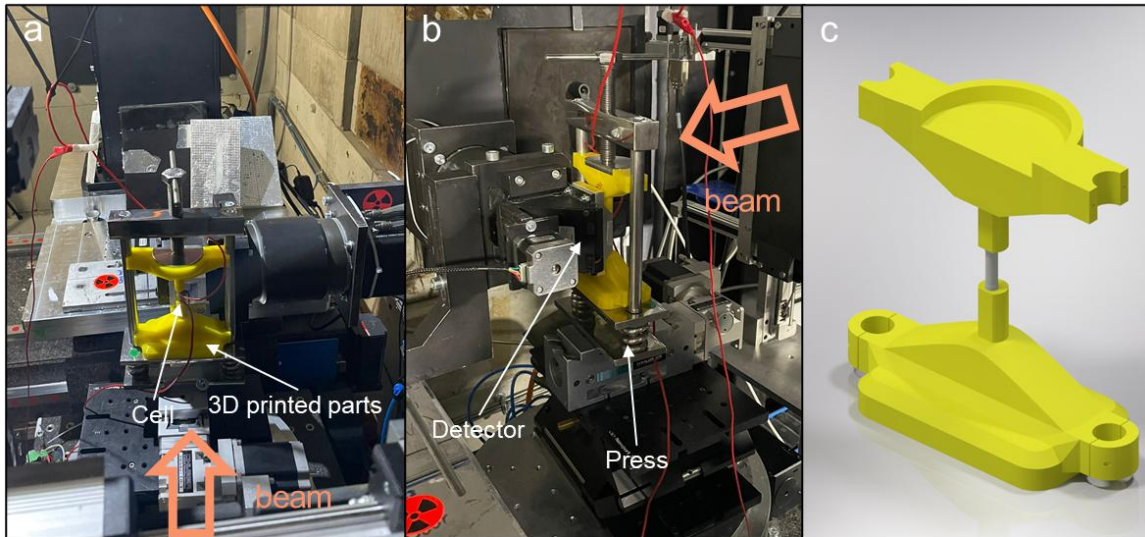
6 1. *Univ. Grenoble Alpes, Univ. Savoie Mont Blanc, CNRS, Grenoble INP, LEPMI, 38000*
7 *Grenoble, France*

8 2. *Institut Laue-Langevin, 71 Avenue des Martyrs, 38000 Grenoble, France*

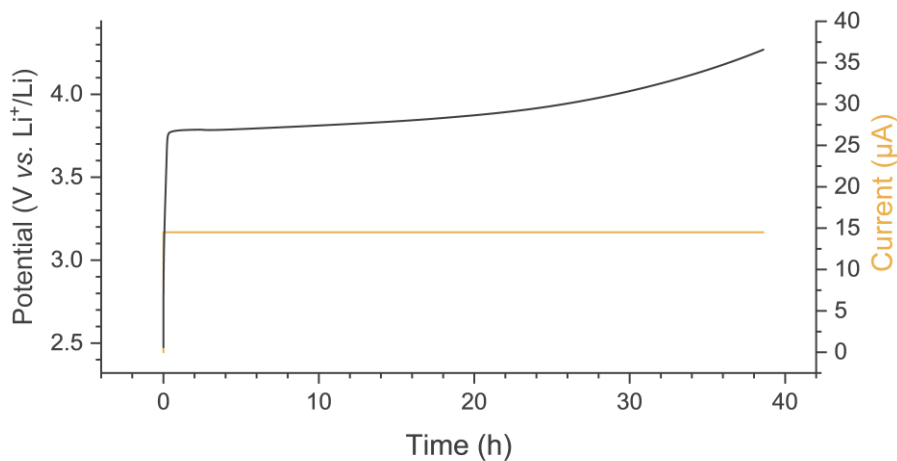
9

10 **Corresponding Author**

11 * E-mail: patrice.perrenot@grenoble-inp.fr; claire.villevieille@grenoble-inp.fr



12
 13 **Figure S1:** Pictures of the experimental setup at NeXT instrument in a) the same direction of the beam
 14 and b) a side view. c) the 3D printed frame that it fixed in the modified dental press, which allowed high
 15 spatial resolution neutron radiography imaging.



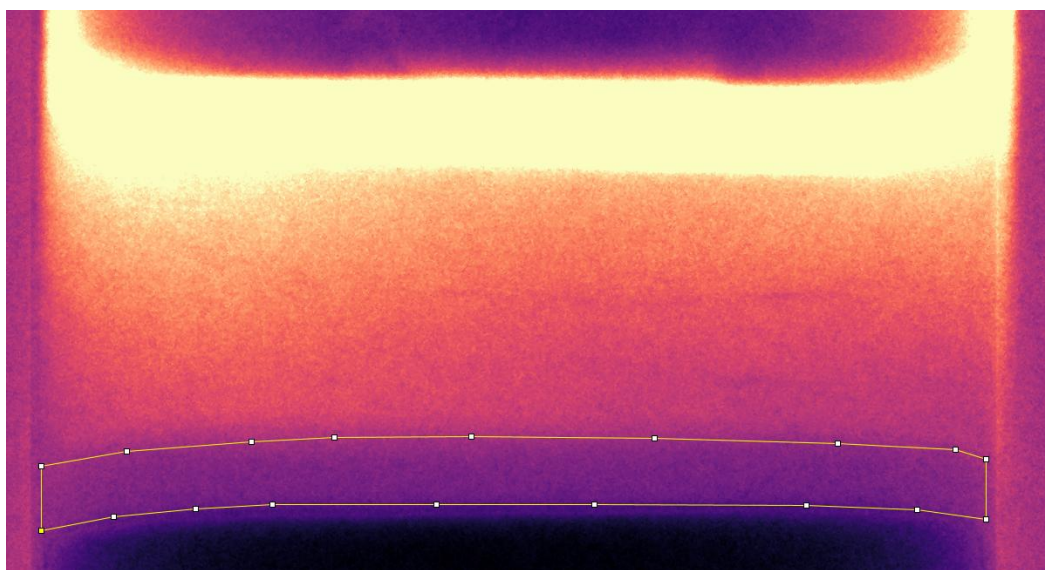
16
 17 **Figure S2:** First charge of the cell (NMC532 vs. In⁶Li_{0.3}, with LPSCl as a solid electrolyte) cycled at a
 18 C/40 rate and 25°C in the laboratory between 2.5 to 4.3 V vs Li⁺/Li.

19 **Note S1. Concentration calculations**

20 **a. Pristine state**

21 Since the composite electrode is made of natural Li as well as the solid electrolyte, we can
22 expect to have a natural ${}^6\text{Li}/{}^7\text{Li}$ exchange between the counter electrode made of $\text{In}{}^6\text{Li}$ and the
23 rest of the cell made of natural Li (considering that natural Li is made of 92.6% of ${}^7\text{Li}$ and 7.4%
24 of ${}^6\text{Li}$). Thus, when starting the *operando* imaging measurement, we can “easily” calculate the
25 ${}^6\text{Li}$ concentration of the CE since (i) the concentration is known from the weighed cell
26 fabrication, (ii) it has been enriched to an exact concentration of ${}^6\text{Li}$, and (iii) that the self-
27 diffusion from the $\text{In}{}^6\text{Li}$ to the positive electrode through the thick electrolyte is neglectable at
28 the pristine state (initial time t_0) and that the cell was also charged without being set to rest for a
29 long period.

30 The quantity of lithium has been calculated from the weights during the sample fabrication (n_{Li}
31 $_{\text{tot}}$). The volume occupied by the cell components, and in particular the CE, has been measured
32 on the images, as a clear distinction between the CE and the separator can be seen. The
33 projection area of the composite electrode has been measured using Fiji software³⁹ as follows:



34

35 **Figure S3:** Measurement of the projected area (highlighted in yellow) of the positive electrode by
 36 image analysis at the charged state.

37 Then, the volume occupied by the CE has been calculated with the following formula:

$$V = \frac{\pi D}{4} \times A \quad (1)$$

38
 39 With V the volume in cm³, D the diameter in cm, and A the projected surface area in cm²
 40 (highlighted in yellow in **Figure S3**).

41 Taking the lithium natural abundance (⁶Li/⁷Li) at 7.4 %/92.6 % and knowing the quantity of
 42 lithium inside the composite electrode, the concentration can be calculated. The same calculation
 43 can be obtained with the separator and the negative electrode. The values are summed up in
 44 **Table S1**.

45 **Table S1:** Concentration calculation of the pristine state of the composite electrode (CE), the
 46 separator, and the negative electrode.

Metrics in pristine state	Composite electrode (70%w NMC + 30%w LPSCI)	Separator (LPSCI)	Negative electrode (In ⁶ Li)
Mass m _{Li LPSCI} (g)	1.60 x10 ⁻³	1.16 x10 ⁻²	/
Molar mass M _{Li LPSCI} (g/mol)	2.68 x10 ²	2.68 x10 ²	/
Amount of substance n _{LPSCI} (mol)	5.96 x10 ⁻⁶	4.32 x10 ⁻⁵	/
Amount of substance n _{Li LPSCI} (mol)	3.58 x10 ⁻⁵	2.59 x10 ⁻⁴	/
Mass m _{AM} (g)	3.80 x10 ⁻³	/	7.50 x10 ⁻¹
Molar mass M _{AM} (g/mol)	9.66 x10 ¹	/	6.02
Amount of substance n _{Li AM} (mol)	3.94 x10 ⁻⁵	/	1.25 x10 ⁻¹

Pixel size (cm)	2.65×10^{-4}	2.65×10^{-4}	2.65×10^{-4}
Horizontal area A (from image) (pix²)	96714	354429	109017
Horizontal area A (from image) (cm²)	6.79×10^{-3}	2.49×10^{-2}	7.66×10^{-3}
Height h (cm)	2.26×10^{-2}	8.30×10^{-2}	2.55×10^{-2}
Volume V (from image) (cm³)	1.60×10^{-3}	5.86×10^{-3}	1.80×10^{-3}
Amount of substance $n_{\text{Li tot}}$ (mol)	7.51×10^{-5}	2.59×10^{-4}	1.25×10^{-1}
Concentration Li_{tot} (at/cm³)	2.83×10^{22}	2.66×10^{22}	4.16×10^{22}
Concentration ⁶Li (at/cm³)	2.15×10^{21}	2.02×10^{21}	3.95×10^{25}
Concentration ⁷Li (at/cm³)	2.61×10^{22}	2.46×10^{22}	2.08×10^{22}

47

48 **b. Infinite time diffusion**

49 To calculate the infinite time diffusion concentration in each component, the total amount of
50 substance of ⁶Li and ⁷Li is calculated in the entire cell based on the previous calculation in **Table**
51 **S1**. The average content of ⁶Li in the entire cell is calculated, and the final ratio of abundance to
52 infinite time diffusion is determined. This ratio is then used on the amount of substance of the
53 total Li content in each component. The results, presented in **Table 1**, will also be shown in the
54 scheme in **Figure 3**.

55 **c. Charged state**

56 The cell has then been charged in the laboratory, and the composite electrodes have been
57 delithiated. Assuming that every coulomb exchanged during charging is caused by the
58 delithiation of the active materials, and that only Li⁺ can move in the cell, we can determine the
59 quantity of lithium “plated” at the negative electrode ($n_{\text{Li electrochem plated}}$) using the Faraday’s law.
60 As the composite electrode is being delithiated, this amount can be subtracted from the previous

61 amount of lithium $n_{Li\ AM}$ calculated in **Table S1** for the composite electrode to obtain the lithium
 62 concentration after the first charge.

63 **Table S2:** Concentration calculation at the delithiated state of the composite electrode.

Charged composite electrode (CE): delithiated state (70%w NMC + 30%w LPSCI)	
Metrics	Value
n_{Li} electrochem plated (mol)	2.19×10^5
$n_{Li\ CE}$ delithiated (mol)	5.32×10^5
$at_{Li\ CE}$ delithiated (at)	3.20×10^{19}
Concentration Li_{CE} delithiated (at/cm³)	2.00×10^{22}
Concentration ${}^6Li_{CE}$ delithiated (at/cm³) (7.4 %)	1.50×10^{21}
Concentration ${}^7Li_{CE}$ delithiated (at/cm³) (92.6 %)	1.85×10^{22}

64

65 **d. Charged state (beginning of the neutron experiment)**

66 The cell has then been placed in the beam line. The dark and flat field images have been taken,
 67 and the neutron radiography acquisition has been started while the cell is being discharged. Once
 68 again, considering that every coulomb is only dedicated to the lithiation/delithiation of the
 69 composite electrode, we can determine the quantity of lithium reinserted in the composite
 70 electrode ($n_{Li\ electrochem\ stripped}$). Hence, this amount can be added to the previous amount of lithium
 71 $n_{Li\ CE\ delithiated}$ corresponding to the delithiated state, calculated in **Table S2**. However, in the
 72 relithiation, due to the enriched negative electrode with 6Li and the exchange of ${}^6Li/{}^7Li$ that
 73 could have happened between the negative electrode and the separator, the reinserted Li^+ in the
 74 NMC may not be in the same ratio as the natural abundance of lithium isotopes.

75 **Table S3:** Concentration calculation at the relithiated state of the composite electrode.

Recharged composite electrode: relithiated state (70%w NMC + 30% w LPSCI)	
Metrics	Value
n_{Li} electrochem discharge (mol)	1.81 x10 ⁵
n_{Li} CE relithiated (mol)	8.89 x10 ⁵
at_{Li} WE relithiated (at)	5.35 x10 ¹⁹
Concentration Li_{WE} lithiated (at/cm³)	3.35 x10 ²²
Concentration ⁶Li_{WE} lithiated (at/cm³) (7.4 %)	2.51 x10 ²¹
Concentration ⁷Li_{WE} lithiated (at/cm³) (92.6 %)	2.32 x10 ²¹

76

77 **Note S2. Quasi-stationary state of transport during charging through the separator**

78 The majority of ⁶Li in the system is present in the In⁶Li negative electrode at the pristine (n_{6Li}
79 neg. elec.), as opposed to the natural abundance in the rest of the cell. When a gradient of
80 concentration is present, ⁶Li will diffuse in different ^{nat}Li materials^{40,41}. During the charge, when
81 transport processes are in opposite direction, the ⁶Li concentration along the separator is at a
82 quasi-stationary state (Figure 5). In other words, the total ⁶Li flux is equal to zero indicating that
83 the flux of isotopic diffusion and of the electrochemical migration are counterbalancing each
84 other and can be considered as equal during the charge. The following equation describe this
85 state:

$$J_{diff} = -J_{migr} \quad (2)$$

86 **Conduction associated to ⁶Li in the separator**

87 As we are only following the ⁶Li isotope with the neutron radiography, we need to determine
88 the associated average enrichment of ⁶Li along the separator.

89 The average ${}^6\text{Li}$ concentration during the charge is measured along the separator at 3.28×10^{21}
 90 at/cm^3 . Compared to the initial calculated value of ${}^6\text{Li}$ concentration in the separator (2.02×10^{21}
 91 at/cm^3), this corresponds to an average 12% of ${}^6\text{Li}$ enrichment.

92 The electrochemical migration flux is defined by the equation that follows:

$$J_{migr} = \frac{Z {}^6\text{Li} F}{RT} D {}^6\text{Li} C {}^6\text{Li} \frac{\partial \varphi(x)}{\partial x} = \mu {}^6\text{Li} C {}^6\text{Li} \frac{\Delta E}{L} = \frac{\sigma_{LPSCl} \times x {}^6\text{Li}}{e} \frac{\Delta E}{L} \quad (3)$$

93
 94 With σ_{LPSCl} the ionic conductivity of LPSCl (S/cm), $x_{6\text{Li}}$ the fraction of ${}^6\text{Li}$ enrichment, e the
 95 elementary charge (in C), ΔE the potential difference between the positive and negative electrode
 96 (in V) and L the length of the separator (in cm).

97 Based on equations (2) and (3), the following equality can be written:

$$J_{diff} = D {}^6\text{Li} \frac{\partial C}{\partial x} = -J_{migr} \quad (4)$$

98 By ordering equation (4), the diffusion coefficient can be calculated as follows:

$$D {}^6\text{Li} = -J_{migr} \times \frac{\partial x}{\partial C} \quad (5)$$

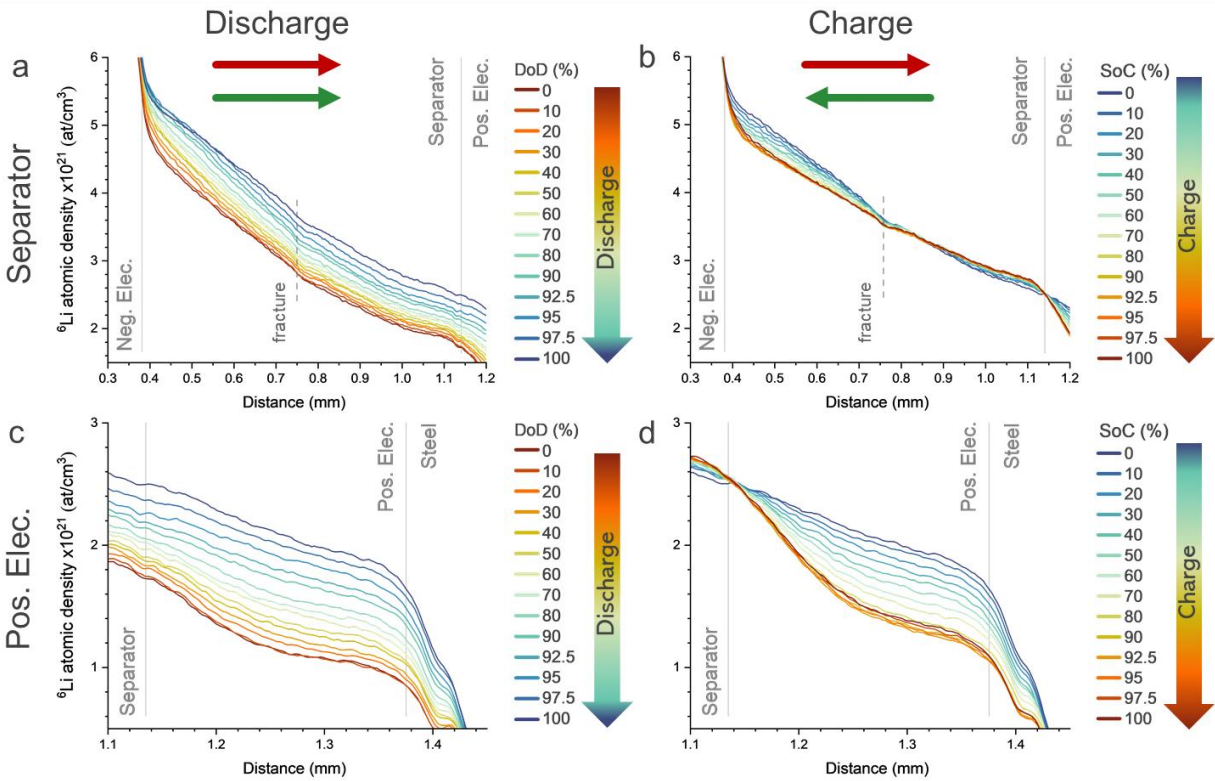
99 The data are available in **Table S4**.

100 **Table S4:** Diffusion coefficient calculation based on the equivalent electrochemical migration.

Diffusion calculation	
Metrics	Value
$x_{6\text{Li}}$	12×10^{-2}
$\sigma_{6\text{Li}}$ (S/cm)	2×10^{-3}
e (C)	1.602×10^{-19}
ΔE (V)	3.26
L (cm)	8.3×10^{-2}

J_{migr} (at/cm ² ·s)	5.88×10^{16}
$\partial C/\partial x$ (at/cm ⁴)	2.43×10^{22}
$D_{6\text{Li}}$ in ${}^7\text{LiPSCl}$ (cm ² /s)	2.42×10^{-6}

101



102

103 **Figure S4:** Profiles of ⁶Li content along the cell components at different DoD and SoC during

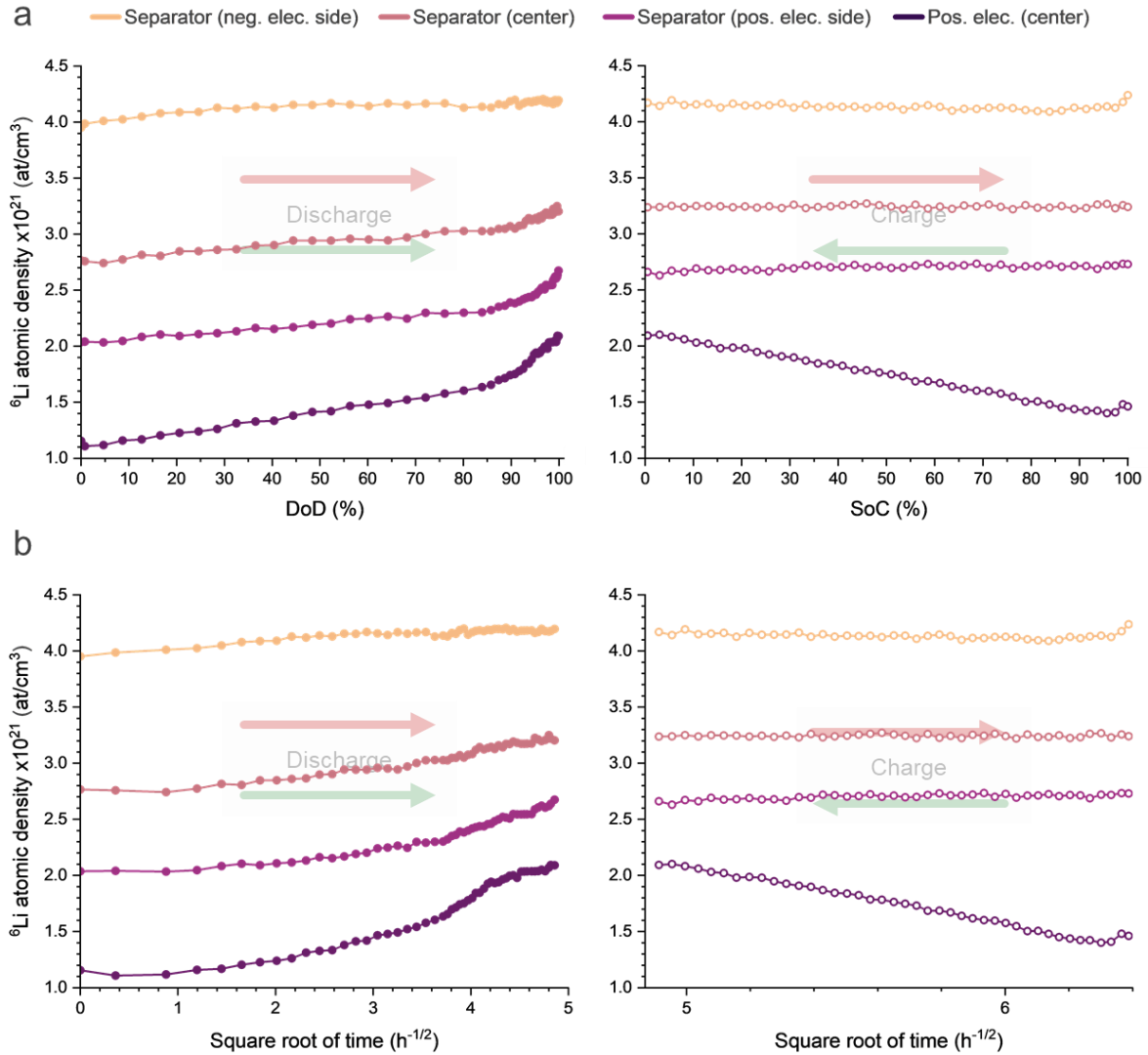
104 a, c) discharge and b, d) charge, averaged over the entire width of the sample. The top panels

105 focus on the separator and the bottom panels focus on the positive electrode, respectively. The

106 red and green arrows highlight the direction of the isotopic diffusion and the electrochemical

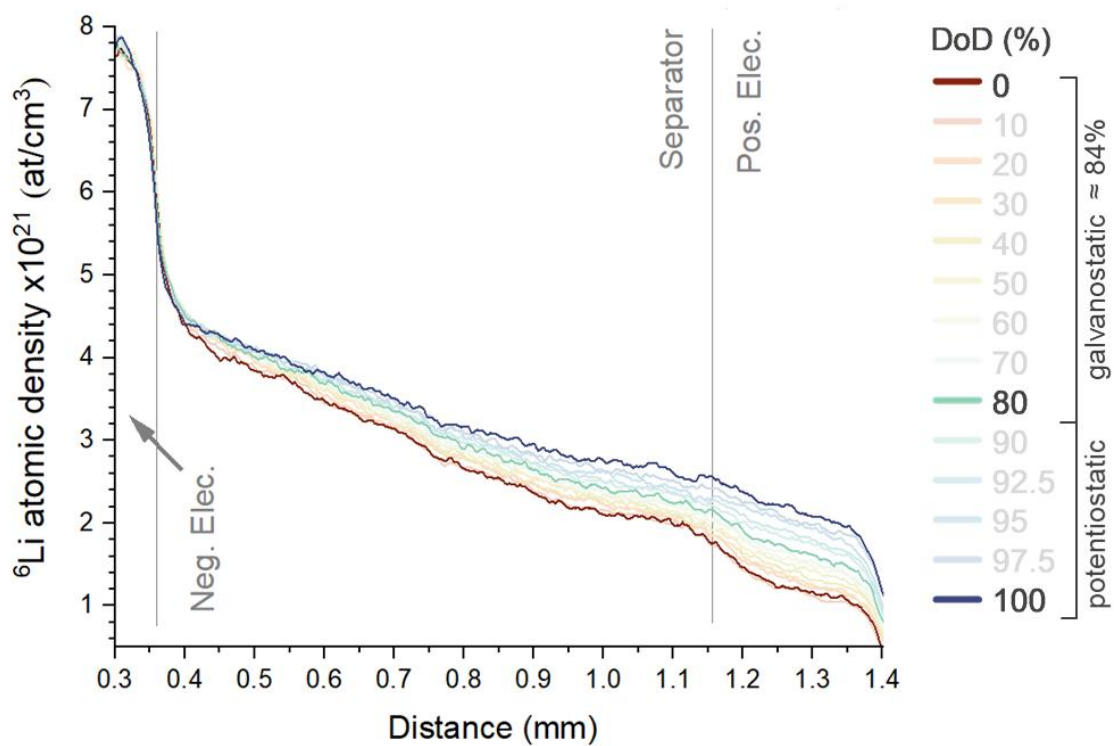
107 migration, respectively. The dashed line indicates the position of an identified fracture. The

108 arrows on the right help visualize the curves' evolution during cycling.



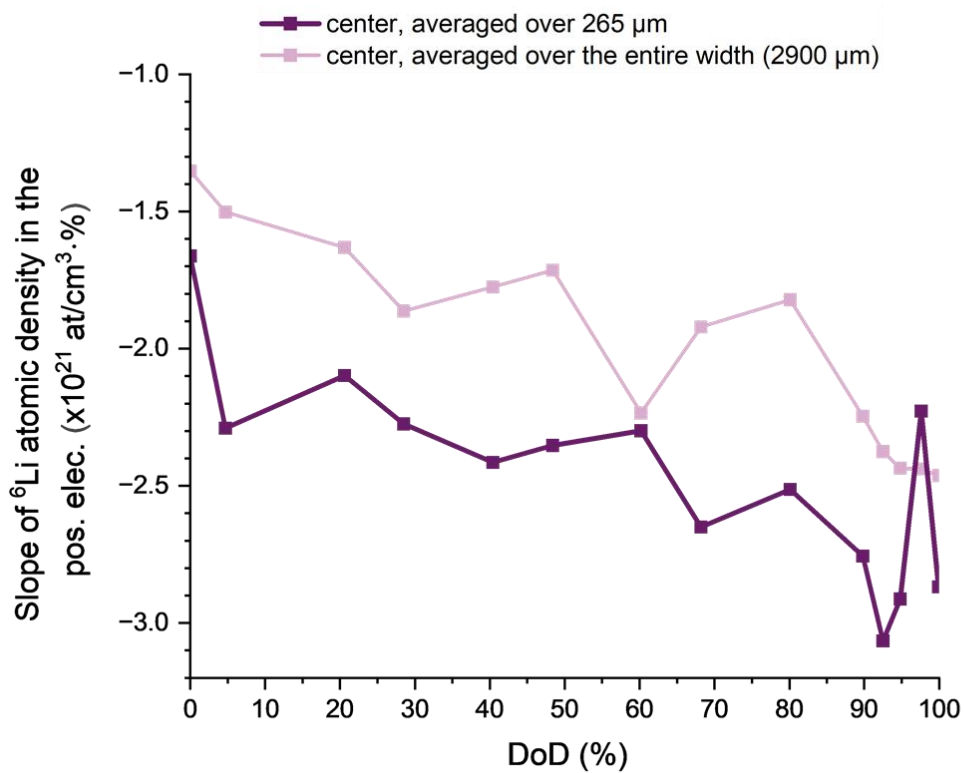
109

110 **Figure S5:** ^6Li atomic density as function of a) DoD and SoC and b) the square root of time at various
 111 height in the separator and in the positive electrode, measured in the center over a width of $265\ \mu\text{m}$,
 112 highlighting diffusion-driven transport. The red and green arrows refer to the direction of the isotopic
 113 diffusion and the electrochemical migration, respectively. These concepts are further explained in
 114 “Isotopic diffusion vs. electrochemical migration”.



115

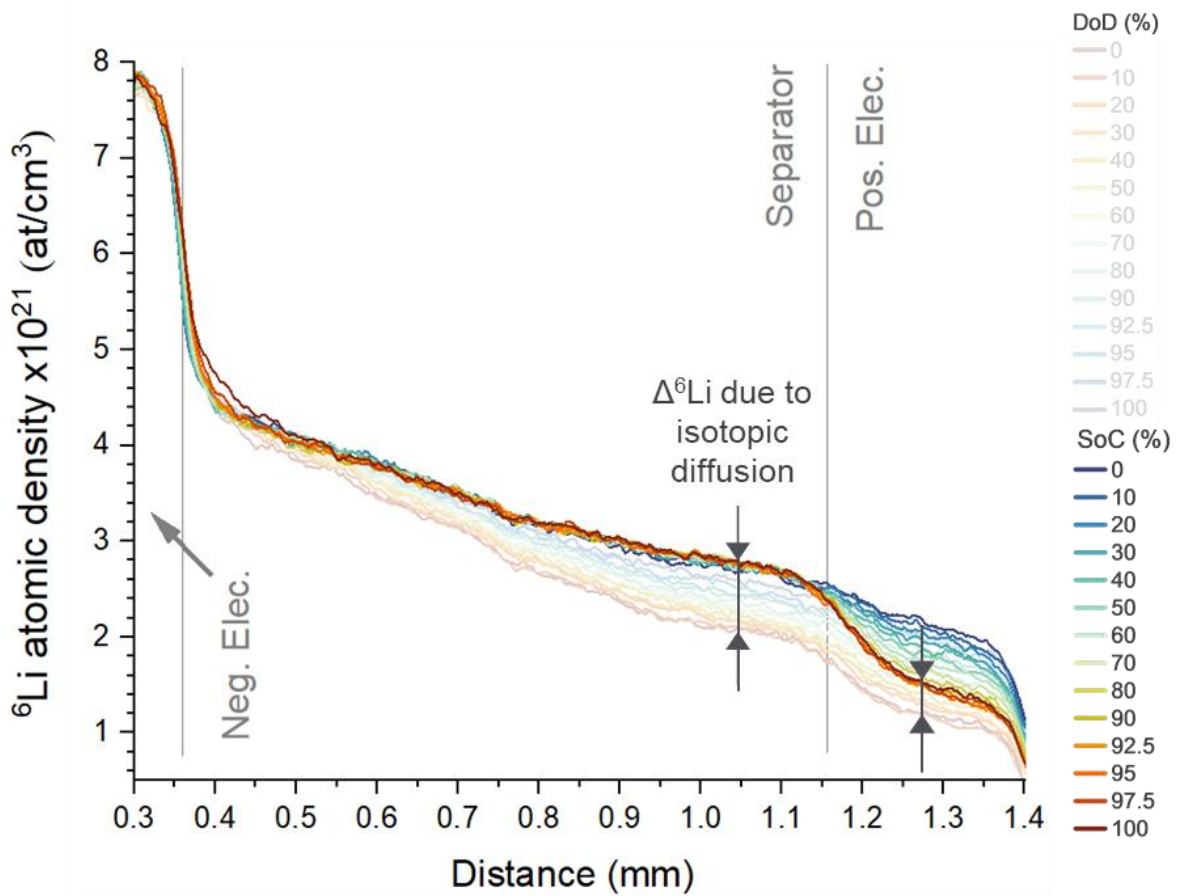
116 **Figure S6:** Profiles of lithium content along the cell components at different DoD, averaged over the
 117 width of the 265 μm , with the highlight of the switch from galvanostatic to potentiostatic regime (at DoD
 118 84%).



119

120 **Figure S7:** Slope of the linear fit in the positive electrode of the ${}^6\text{Li}$ atomic density in function of the DoD,

121 extracted from **Figure 4** and **Figure S4**.

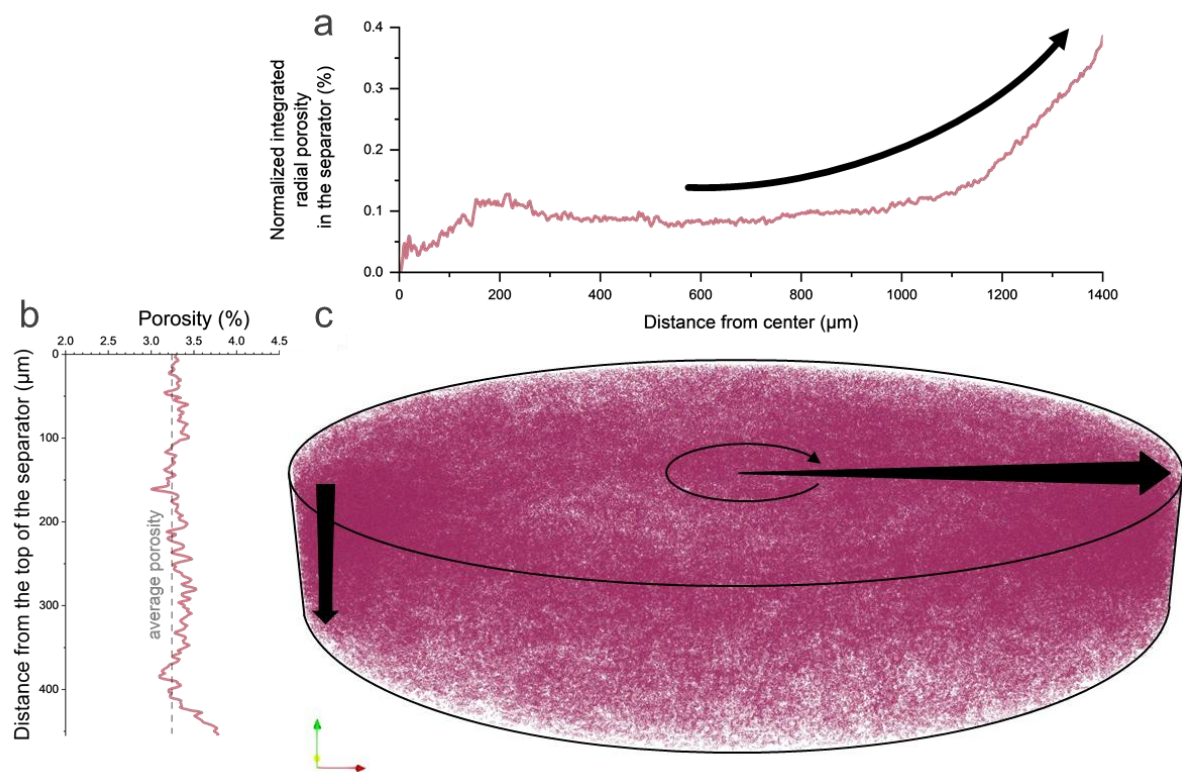


122

123 **Figure S8:** ${}^6\text{Li}$ profiles of lithium content at different DoD and SoC, averaged over the width of the

124 sample, highlighting the evolution of ${}^6\text{Li}$ due to isotopic diffusion in the separator and the positive

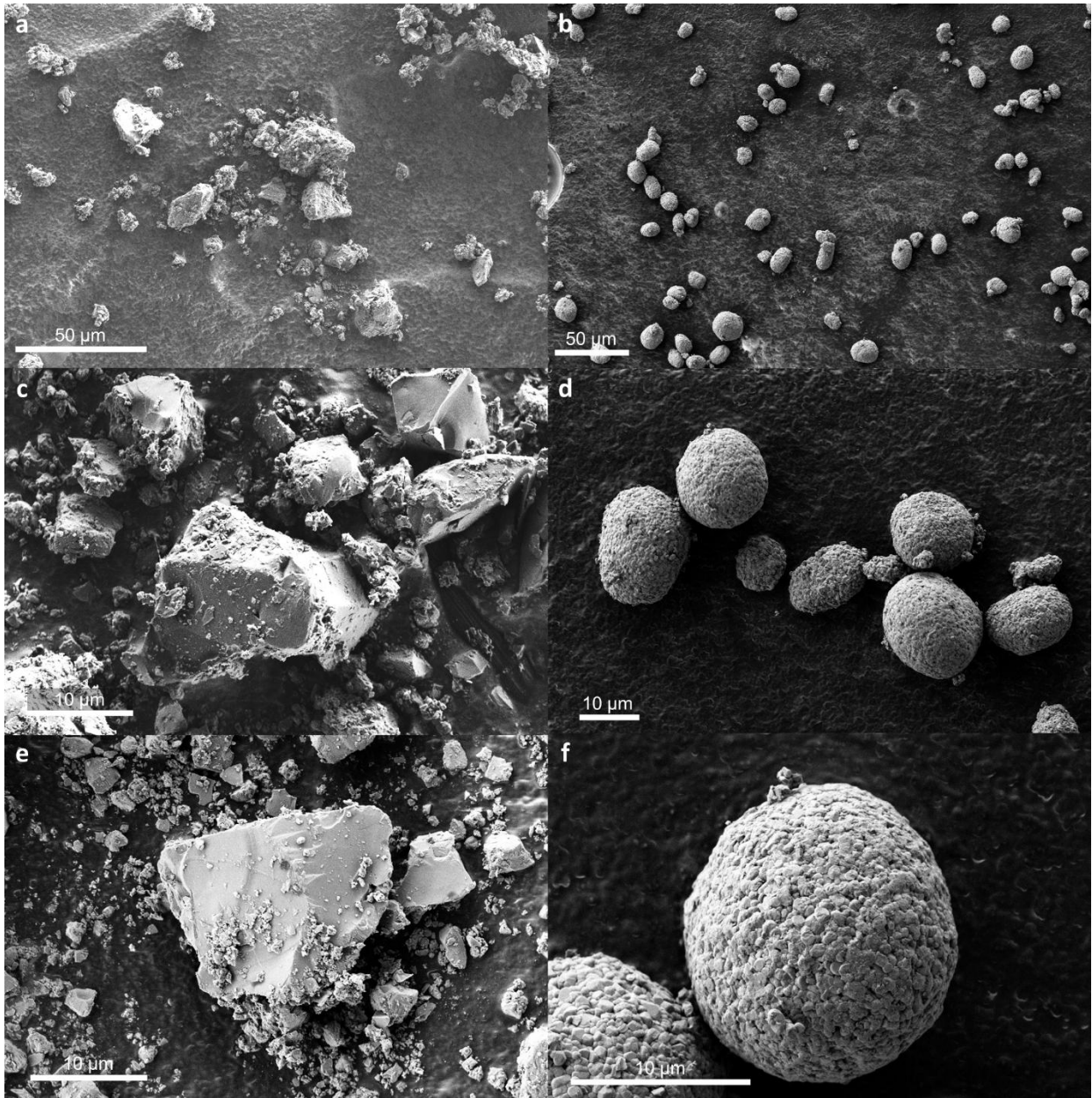
125 electrode as the cell come back to its original state of SoC 100%.



126

127 **Figure S9:** Spatial distribution measurement of porosity made at ID19 (ESRF) on LPSCI separator. a) the
 128 integrated radial distribution of porosity, highlighting higher porosity on the edge of the sample. b) the
 129 height-wise distribution per slice of porosity, showing homogeneous porosity along the height of the
 130 separator. c) 3D representation of the porosity in the LPSCI separator with the pellet diameter of 3 mm with

131 the arrows in the center showing the radial integration and the arrow on the side showing the height-wise
132 measurement.



133
134 **Figure S10:** Secondary electrons images of a), c), e) the LPSCl powder and b), d), f) the NMC532
135 powder.